SANDIA REPORT
SAND2012-10690
Unlimited Release
Printed January 2013

Earth Curvature and Atmospheric Refraction Effects on Radar Signal Propagation

Armin W. Doerry

Prepared by
Sandia National Laboratories
Albuquerque, New Mexico 87185 and Livermore, California 94550

Sandia National Laboratories is a multi-program laboratory managed and operated by Sandia Corporation, a wholly owned subsidiary of Lockheed Martin Corporation, for the U.S. Department of Energy's National Nuclear Security Administration under contract DE-AC04-94AL85000.

Issued by Sandia National Laboratories, operated for the United States Department of Energy by Sandia Corporation.

Available to DOE and DOE contractors from

U.S. Department of Energy
Office of Scientific and Technical Information
P.O. Box 62
Oak Ridge, TN 37831

Telephone: (865) 576-8401
Facsimile: (865) 576-5728
E-Mail: reports@adonis.osti.gov
Online ordering: http://www.osti.gov/bridge

Available to the public from

U.S. Department of Commerce
National Technical Information Service
5285 Port Royal Rd.
Springfield, VA 22161

Telephone: (800) 553-6847
Facsimile: (703) 605-6900
E-Mail: orders@ntis.fedworld.gov
Online order: http://www.ntis.gov/help/ordermethods.asp?loc=7-4-0#online

SAND2012-10690
Unlimited Release
Printed January 2013

Earth Curvature and Atmospheric Refraction Effects on Radar Signal Propagation

Armin W. Doerry
ISR Mission Engineering
Sandia National Laboratories
Albuquerque, NM 87185-0519

Abstract

The earth isn't flat, and radar beams don't travel straight. This becomes more noticeable as range increases, particularly at shallow depression/grazing angles. This report explores models for characterizing this behavior.

Acknowledgements

The production of this report is a result of an unfunded Internal Research and Development effort.

Contents

Foreword

This report is an updated and enhanced version of a previous limited distribution report.[1] The distribution limitation of the earlier report was limited to “Internal Distribution” merely because of the publication vehicle being an Internal Memorandum, chosen at the time arbitrarily, with no other particular reason for restricting its Unlimited Release.

This report details the results of an academic study. It does not presently exemplify any modes, methodologies, or techniques employed by any operational system known to the authors.

The specific mathematics and algorithms presented herein do not bear any release restrictions or distribution limitations.

This distribution limitations of this report are in accordance with the classification guidance detailed in the memorandum “Classification Guidance Recommendations for Sandia Radar Testbed Research and Development”, DRAFT memorandum from Brett Remund (Deputy Director, RF Remote Sensing Systems, Electronic Systems Center) to Randy Bell (US Department of Energy, NA-22), February 23, 2004. Sandia has adopted this guidance where otherwise none has been given.

This report formalizes preexisting informal notes and other documentation on the subject matter herein.

1 Introduction

The question that we ultimately seek to answer is “To see a given range, or range swath, just where exactly do we point the antenna?” Furthermore we ask “Just what exactly is the grazing angle at the target?”

The typical assumption for many radar systems is that the earth is sufficiently flat so that the depression angle at the aircraft is the same as the grazing angle at the target. While this isn’t too bad for relatively low-flying aircraft and relatively near-range geometries, it falls apart as ranges approach the radar horizon from higher altitudes. In space it is imperative to account for earth curvature.

Ultimately, we expect the utility of this analysis to be in facilitating antenna pointing to optimize radar echo Signal-to-Noise Ratio (SNR) for a desired range swath, particularly at long ranges and shallow depression angles. Herein we concern ourselves strictly with the refraction and curved earth phenomena. Application to optimizing SNR for a particular range swath will be deferred to a future report.

Another aspect of refraction is its influence on radar echo timing, and ultimately ranging accuracy via the velocity of propagation. This aspect is beyond the scope of this report and will be deferred to a subsequent report.

2 The Basic Equations

The modifications to geometry and trigonometry equations for including earth curvature aren't too bad, especially when we consider the earth as spherical in nature, which is reasonable for the task at hand. Consider the situation in Figure 1. Parameters are defined as

R_e = radius of the earth, nominally 6378 km,
h_a = altitude of aircraft,
R = range from aircraft to surface target,
ϕ_e = earth surface angular change,
ψ_d = depression angle at aircraft (positive below horizontal), and
ψ_g = grazing angle at target (positive above horizontal). (1)

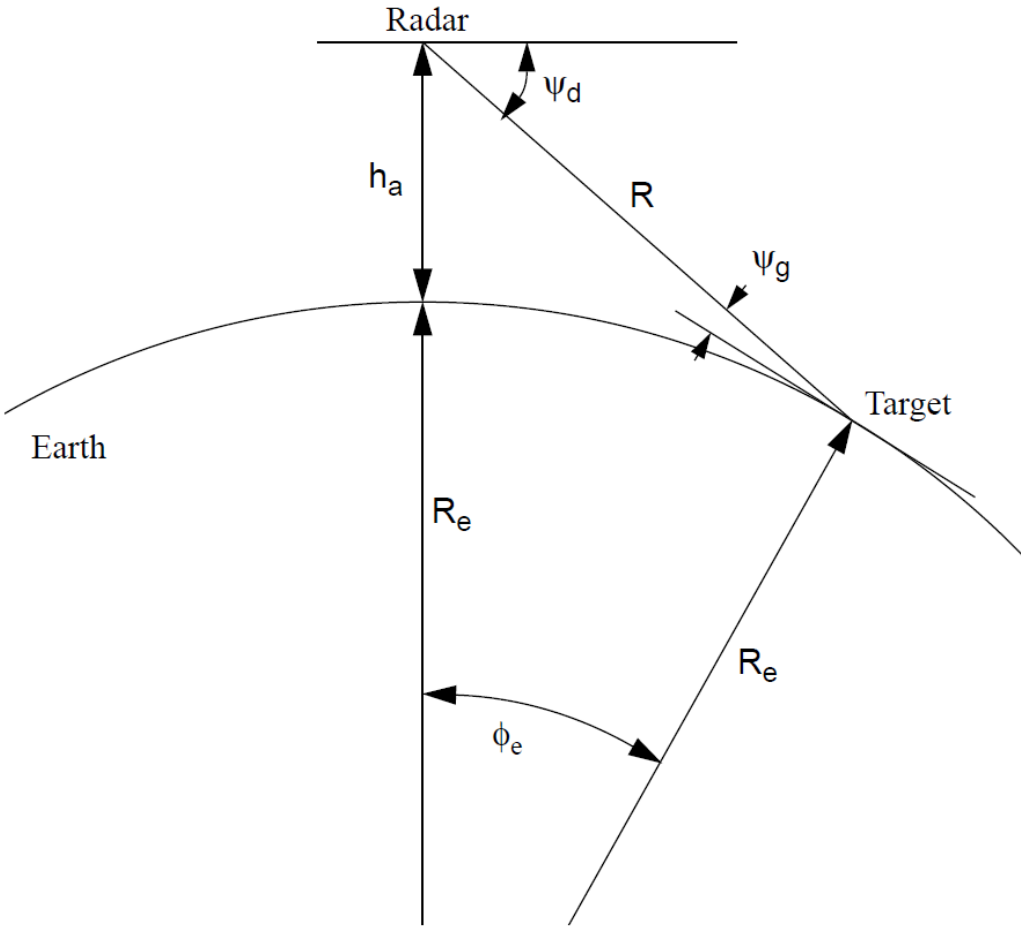

Figure 1. Spherical earth geometry.

2.1 Line-of-sight Propagation

Finding the appropriate angles from the various distance measures is an exercise in the application of the Law of Cosines for planar triangles.

Assuming that propagation is line-of-sight, the appropriate angles are calculated to be

$$\sin\psi_d = \frac{h_a}{R}\left(1-\frac{h_a}{2(R_e+h_a)}\right)+\frac{R}{2(R_e+h_a)},$$
$$\sin\psi_g = \frac{h_a}{R}\left(1+\frac{h_a}{2R_e}\right)-\frac{R}{2R_e}, \text{ and}$$
$$\cos\phi_e = 1-\frac{\left(R^2-h_a^2\right)}{2R_e(R_e+h_a)}. \tag{2}$$

In addition, we know that for this trigonometry

$$\phi_e = \psi_d - \psi_g. \tag{3}$$

Furthermore, the range *R* can be calculated as

$$R = (R_e+h_a)\sin\psi_d - \sqrt{R_e^2-(R_e+h_a)^2\cos^2\psi_d}, \text{ or}$$
$$R = -R_e\sin\psi_g + \sqrt{R_e^2\sin^2\psi_g + 2R_eh_a + h_a^2}. \tag{4}$$

The arc length along the earth's surface between nadir and the target is given by

$$d = R_e\phi_e. \tag{5}$$

The presumption for all of this, of course, is that the radar beam propagates along the line-of-sight from aircraft to target. Unfortunately, this is wrong, or at best not quite right.

A secondary presumption here is that the earth is spherical. This is also not strictly correct, but is good enough for the purposes of this report. It should be noted that typical radar systems presume an ellipsoidal earth for navigation and pointing, but with line-of-sight propagation also for pointing the antenna.

2.2 Non-line-of-sight Propagation

The atmosphere is not homogeneous and usually causes the radar energy to bend towards the earth, much like a lens. This refraction allows the radar to 'see' beyond the horizon somewhat. A common 'trick' is to account for this by presuming the earth possessing a larger radius than it really has, by some factor *k*. Often a factor of $k = 4/3$ is used. Consequently, depression and grazing angles are calculated as

$$\sin\psi_d = \frac{h_a}{R}\left(1 - \frac{h_a}{2(kR_e + h_a)}\right) + \frac{R}{2(kR_e + h_a)}, \text{ and}$$
$$\sin\psi_g = \frac{h_a}{R}\left(1 + \frac{h_a}{2kR_e}\right) - \frac{R}{2kR_e}. \tag{6}$$

Note that $k = 4/3$ is merely a convenient approximation, and that the perfect value for *k* will change somewhat with altitude, atmospheric conditions, frequency, etc.[2] Note also that a flat earth is essentially the case where $k \to \infty$.

The propagation path range can be estimated from the angles as

$$R = (kR_e + h_a)\sin\psi_d - \sqrt{(kR_e)^2 - (kR_e + h_a)^2\cos^2\psi_d}\ , \text{ or}$$
$$R = -kR_e\sin\psi_g + \sqrt{(kR_e)^2\sin^2\psi_g + 2kR_eh_a + h_a^2}\ . \tag{7}$$

We now define the increased earth-radius model earth-radius angular change as

$$\phi'_e = \psi_d - \psi_g\,, \tag{8}$$

and note that

$$\cos(\phi'_e) = 1 - \frac{\left(R^2 - h_a^2\right)}{2kR_e(kR_e + h_a)}, \tag{9}$$

We will assume that the surface distance of the increased earth-radius model is reasonably and acceptably equivalent to that of the actual earth-radius model. Consequently, the arc length along the earth's surface between nadir and the target is given by

$$d \approx kR_e\phi'_e\,. \tag{10}$$

2.3 Elevated Target Surface

If the target surface is at a non-zero altitude above the surface of the spherical earth, then the equations are modified to

$$\sin\psi_d = \frac{(h_a - h_s)}{R}\left(1 - \frac{(h_a - h_s)}{2(kR_e + h_a)}\right) + \frac{R}{2(kR_e + h_a)},$$

$$\sin\psi_g = \frac{(h_a - h_s)}{R}\left(1 + \frac{(h_a - h_s)}{2(kR_e + h_s)}\right) - \frac{R}{2(kR_e + h_s)}, \text{ and}$$

$$\cos(\phi_e') = 1 - \frac{R^2 - (h_a - h_s)^2}{2(kR_e + h_s)(kR_e + h_a)}. \tag{11}$$

where h_s = target surface altitude, and as before

$$\phi_e' = \psi_d - \psi_g\,. \tag{12}$$

Furthermore,

$$R = (kR_e + h_a)\sin\psi_d - \sqrt{(kR_e + h_s)^2 - (kR_e + h_a)^2\cos^2\psi_d}\,, \text{ or}$$

$$R = -(kR_e + h_s)\sin\psi_g + \sqrt{(kR_e + h_s)^2\sin^2\psi_g + 2(kR_e + h_s)(h_a - h_s) + (h_a - h_s)^2}\,. \tag{13}$$

The arc length along the earth's surface between nadir and the target, at the target altitude, is now given by

$$d \approx (kR_e + h_s)\phi_e'. \tag{14}$$

2.4 The Radar Horizon

The radar horizon is defined as that propagation path range *R* that yields a grazing angle $\psi_g = 0$. If we assume an elevated target surface with height h_s, then

$$R_{horizon} = \sqrt{2(kR_e + h_s)(h_a - h_s) + (h_a - h_s)^2} \approx \sqrt{2kR_e h_a} \,. \tag{15}$$

The approximation is for aircraft altitudes much larger than target surface altitude. Note that the propagation path range to the radar horizon will vary as nearly $\sqrt{k}$. This equation is plotted for a k = 4/3 earth model, with $h_s = 0$, in Figure 2.

The corresponding depression angle is

$$\psi_{d,horizon} = \text{acos}\left(\frac{kR_e + h_s}{kR_e + h_a}\right). \tag{16}$$

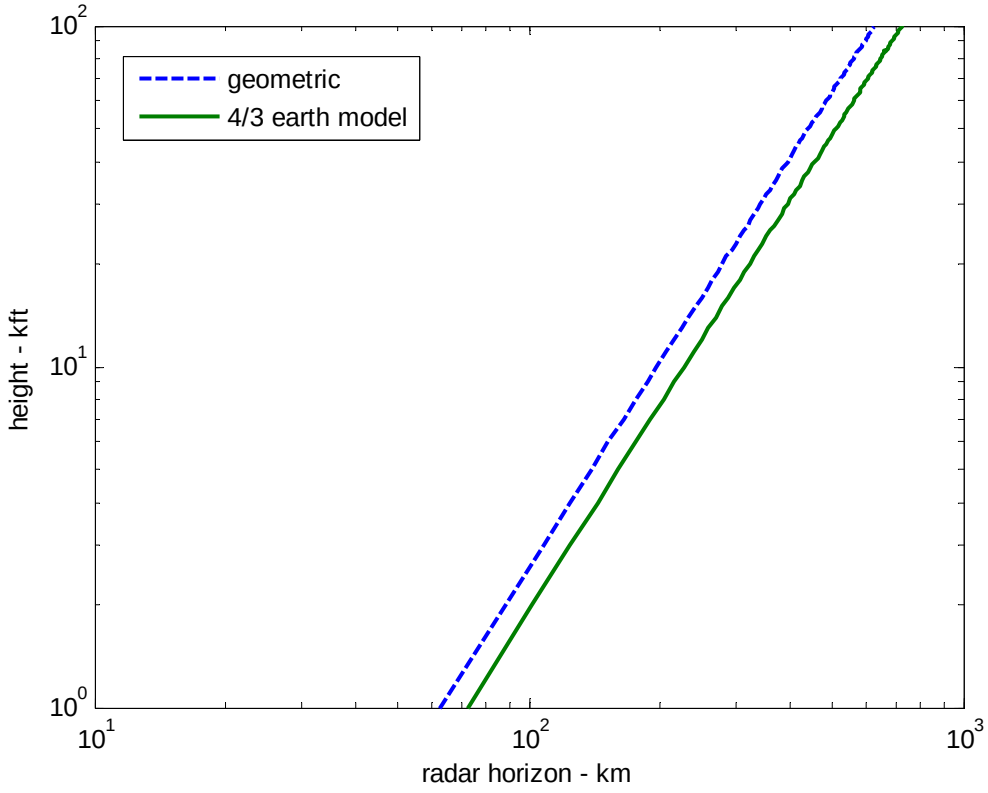

Figure 2. Radar horizon vs. altitude for 4/3 earth model.

2.5 Examples

Consider a sea-level target as seen from an airborne radar at 10 kft altitude. Figure 3 plots the depression angle and grazing angle out to the radar horizon. We note that at the radar horizon, the 4/3 earth model's depression angle differs from the flat earth model's depression angle by about 0.8^{o}, and differs from the geometric depression angle by only about 0.25^{o}. At 10 km, these differences are 0.03^{o} and 0.01^{o} respectively.

Consider a sea-level target as seen from an airborne radar at 25 kft altitude. Figure 4 plots the depression angle and grazing angle out to the radar horizon. We note that at the radar horizon, the 4/3 earth model's depression angle differs from the flat earth model's depression angle by about 1.2^{o}, and differs from the geometric depression angle by only about 0.4^{o}.

Now consider a sea-level target as seen from an airborne radar at 65 kft altitude. Figure 5 plots the depression angle and grazing angle out to the radar horizon. For this geometry, at the radar horizon, the 4/3 earth model's depression angle differs from the flat earth model's depression angle by about 1.95^{o}, and differs from the geometric depression angle by only about 0.65^{o}.

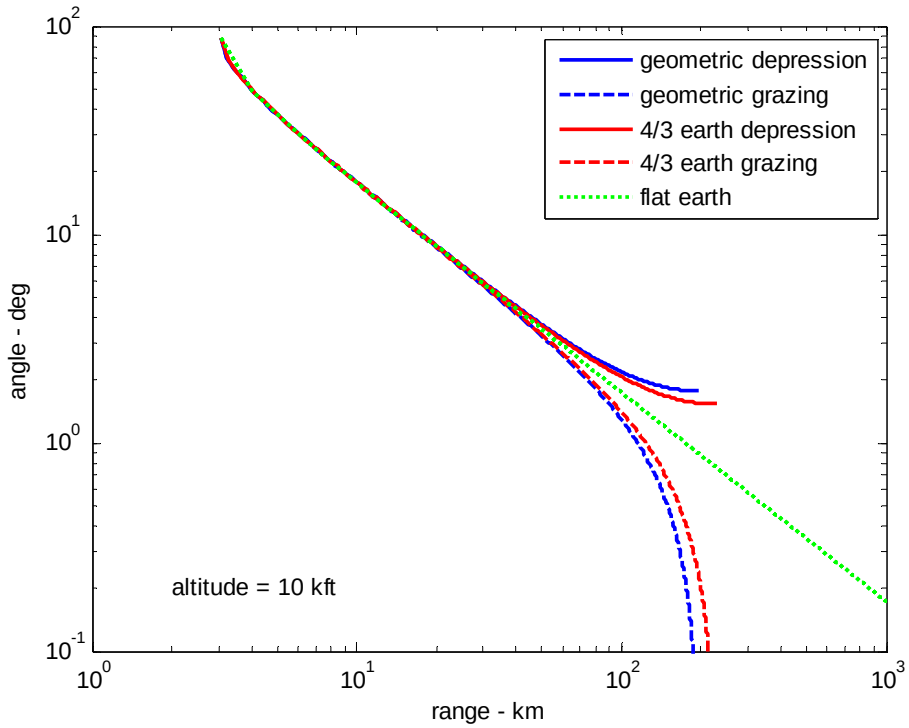

Figure 3. Depression and grazing angles vs. range from 10 kft altitude.

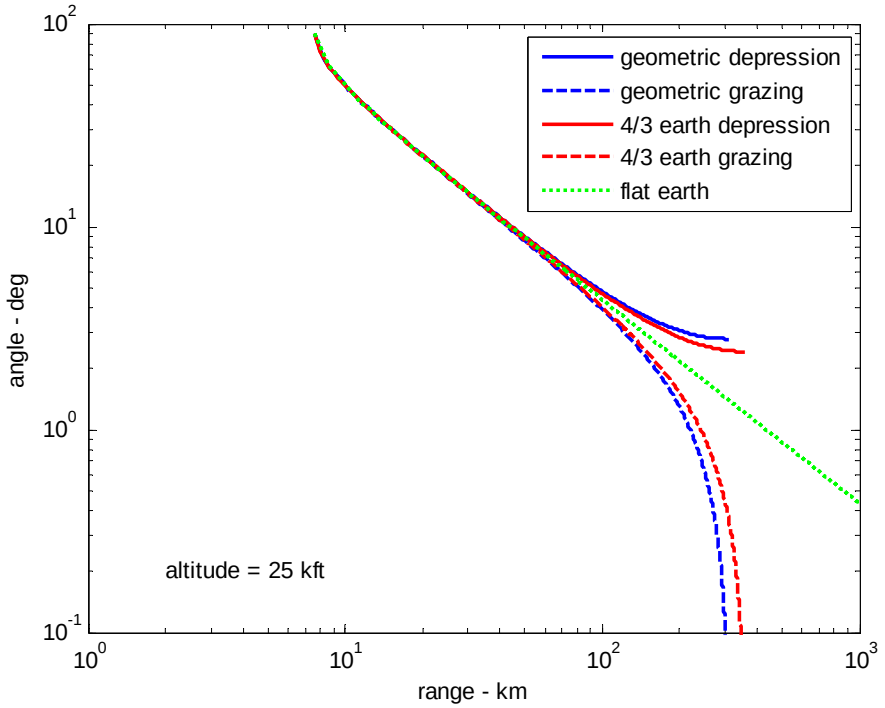

Figure 4. Depression and grazing angles vs. range from 25 kft altitude.

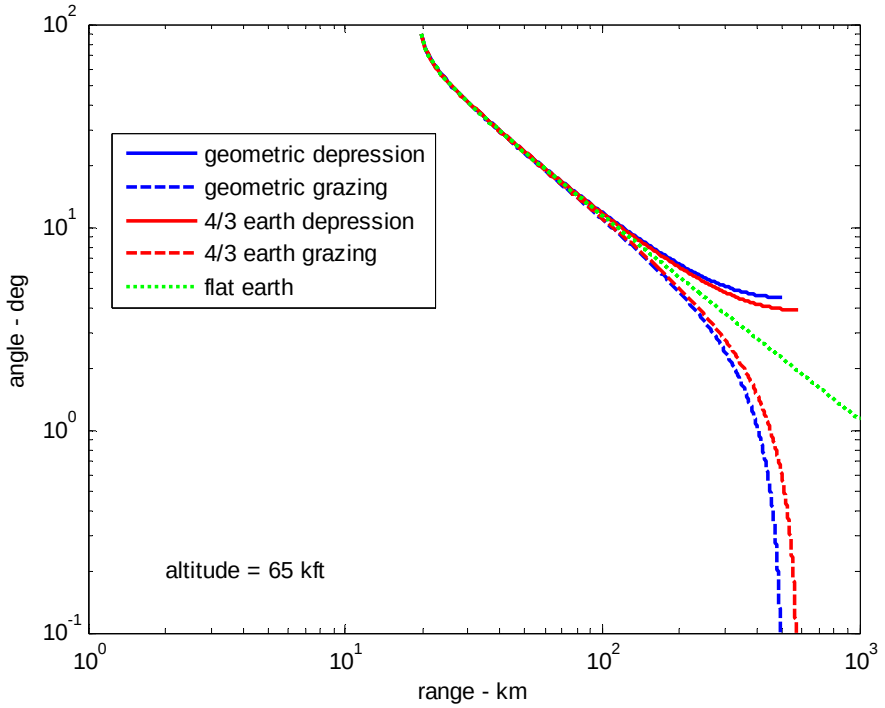

Figure 5. Depression and grazing angles vs. range from 65 kft altitude.

3 More on Refractivity

A common rule of thumb is that atmospheric refractivity is taken care of by $k = 4/3$. While this is useful, it is sort of a ballpark, back-of-the-envelope, squinty-eyed, only sort-of-ok, approximation. It stems from the approximation that the refraction index of the atmosphere is linearly dependent on altitude h with a constant gradient of about $-39.2 \times 10^{-9}\ \mathrm{m}^{-1}$. While reasonable for low altitudes, this isn't quite good enough for typical airborne radar altitudes, not adequately taking into account atmospheric variations and corresponding altitude effects.

We reasonably conclude "There has got to be a better way."

3.1 Refraction vs. Altitude

What we need first is a better appreciation for the effects of the atmosphere, that is, a model for refractivity as a function of atmospheric parameters, including altitude. We offer as general background references a paper by Bean,[3] and a National Bureau of Standards Monograph by Bean and Dutton.[4]

Much has been written in the literature about refraction in the atmosphere for microwave signals. We begin by noting that the index of refraction is often described in terms of N-units, where

$$\begin{aligned} &n = 1 + N\left(10^{-6}\right) \ = \text{index of refraction proper, and} \\ &N = \text{measure of refractivity in N-units.} \end{aligned} \tag{17}$$

Smith and Weintraub[5] present the relationship of refraction at any particular altitude as a function of atmospheric constituents and their respective partial pressure, temperature, etc. Bean and Thayer[6] offer a model of how refractivity changes with altitude. In their model, nature of refractivity is such that on the average it has a fairly linear height gradient to about 1 km above ground, then decays exponentially beyond that. Below an altitude of 9 km, the refractivity depends on surface conditions, which varies with region, season, time of day, etc. Above 9 km, the refractivity is relatively surface-condition independent. We write their segmented model's dependence of refractivity on altitude as

$$N(h) = \begin{cases} N_s + (h - h_s)\Delta N & h_s \le h \le (h_s + 1000\,\mathrm{m}) \\ N_1\, e^{\frac{-(h - h_s - 1000\,\mathrm{m})}{H}} & (h_s + 1000\,\mathrm{m}) \le h \le 9000\,\mathrm{m} \\ 105\, e^{\frac{-(h - 9000)}{7023}} & h > 9000\,\mathrm{m} \quad (\approx 30\,\mathrm{kft}) \end{cases} \tag{18}$$

where

N_s = a measure of refractivity in N-units at the surface,
N_1 = a measure of refractivity in N-units at 1000 m above the surface,
ΔN = refractivity linear decay constant in N-units per meter, and
H = refractivity exponential decay constant in meters. (19)

A minor point is that in this model, height h is with respect to mean sea level. Bean and Thayer offer that the refractivity decay constants can be calculated by

$$\Delta N = -0.00732 e^{0.005577\, N_s} \text{ , and}$$
$$H = \frac{8000 - h_s}{\ln\left(\frac{N_1}{105}\right)} \text{ .} \quad (20)$$

Note that the model for height dependence depends pretty much on surface refractivity. We stress that this is an average model, stipulating that any given atmospheric column might contain significant departures from this, including sharp gradients.[7] Furthermore, optimal calculations for decay constants will vary somewhat regionally.

Surface refractivity varies regionally, and with season and time of day. Various publications by Bean,[3,8] Bean and Dutten,[4] and Bean et al.,[9] show maps that even in the continental US, surface refractivity N_s varies from less than 250 in the mountain west during dry months to over 400 along the south Texas coast in the summer months. An average value for N_s for the continental US is given by Bean as 313.[3] Altshuler[10] reports that his data shows that "the average global surface refractivity is 324.8 N-units and that the standard deviation of [his] sample is 30.1 N-units." Bean and Thayer's segmented model is plotted for several surface refractivity values in Figure 6.

Bean and Thayer also propose a somewhat simpler model for refractivity versus height as

$$N(h) = N_s\, e^{\frac{-(h-h_s)}{H_e}} \text{ ,} \quad (21)$$

where

$$H_e = \frac{1000}{\ln\left(\frac{N_s}{N_s + 1000\Delta N}\right)} \text{, and}$$
$$\Delta N = -0.00732 e^{0.005577\, N_s} \text{ .} \quad (22)$$

They stipulate "This model of atmospheric refractivity is a close representation of the average refractivity structure within the first 3 km." We note, however, that at 30 kft and

for $N_s = 400$ this model differs from the earlier segmented model by 30 N-units. We postulate that a closer approximation over a larger range of altitudes can be found by giving up some accuracy at lower altitudes to gain accuracy at higher altitudes.

We propose to modify the simpler model somewhat, and offer this as

$$N(h) = N_s \, e^{\frac{-(h-h_s)}{H_b}}, \tag{23}$$

where

$$H_b = \frac{h_b - h_s}{\ln\left(\frac{N_s}{N_b}\right)}. \tag{24}$$

In this model, a breakpoint is chosen above 9 km altitude to which the curves converge and pass through. This point is chosen to limit the error between this model and the segmented Bean and Thayer model over some desired range of altitudes. The choice of this point will need to be cognizant of some limited altitude range of interest. For example, over an altitude range of 0 to 50 kft, we might choose

$$\begin{aligned} &h_b = 40\,\text{kft} = 12192\,\text{m}, \text{ and} \\ &N_b = 66.65 \text{ N-units.} \end{aligned} \tag{25}$$

If we were interested in only a range of altitudes between 0 and 30 kft, then we might choose

$$\begin{aligned} &h_b = 30\,\text{kft} = 9144\,\text{m}, \text{ and} \\ &N_b = 102.9 \text{ N-units.} \end{aligned} \tag{26}$$

We do not imply that these models are not useful outside of the ranges of interest used in selecting their parameters, and make no comments on the significance of errors at various altitudes. Furthermore, we stipulate that other factors might at times drive adjustment of these parameters. Nevertheless, we plot the relative error between the simpler Bean and Thayer and the earlier segmented Bean and Thayer model, as well as the relative error between this new simpler model (designed for the altitude range 0-50 kft) and the earlier segmented Bean and Thayer model, in Figure 7. Note that the new simpler model loses some accuracy at the lowest altitudes compared to the simpler Bean and Thayer model, but gains especially above 6 kft or so.

Note that all of this also ignores ‘ducting’, horizontal gradients, boundary layers, and other fine-structure atmospheric phenomena. Furthermore, space-based radars need to include other refraction sources, such as the ionosphere.

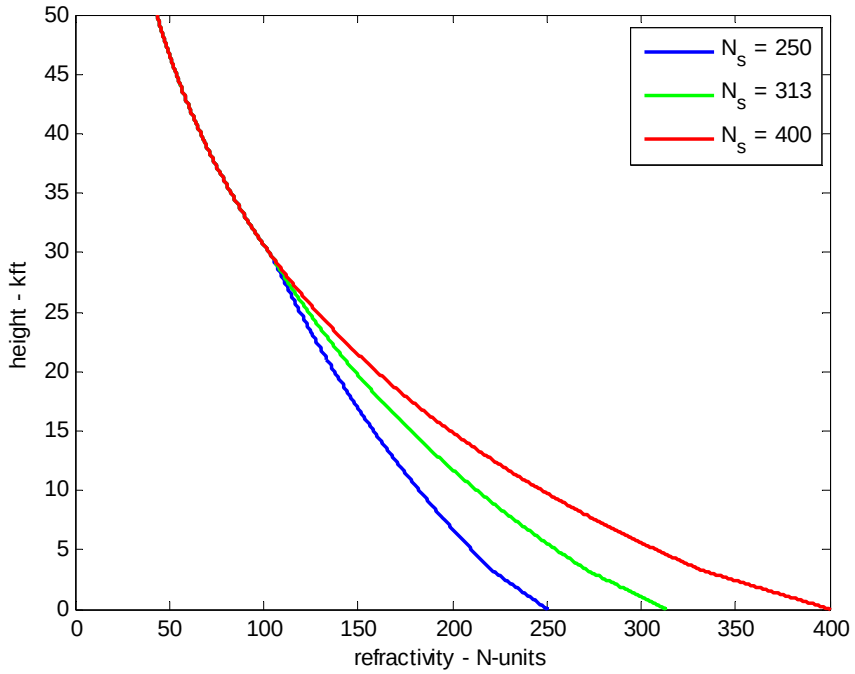

Figure 6. Bean and Thayer's segmented refractivity versus height model.

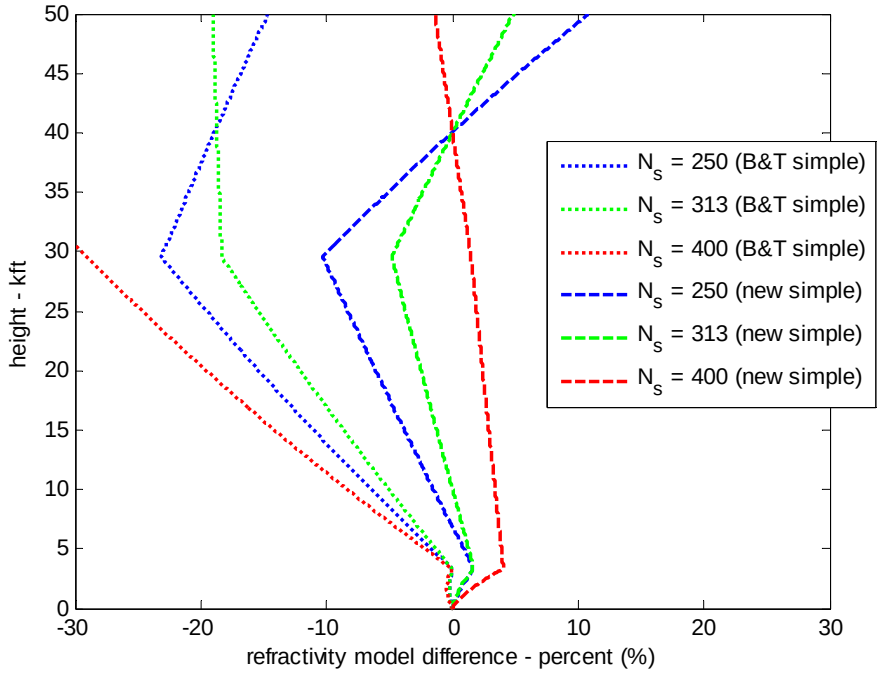

Figure 7. Relative error between simpler models and the segmented Bean and Thayer model, for various surface refractivity values.

3.2 Effective Earth's Radius Models

The radius of curvature for the refraction of a ray is given by[11]

$$\rho \approx \frac{-n}{\left(\frac{dn}{dh}\right)\cos\psi}, \tag{27}$$

where

ψ = instantaneous depression/grazing angle. (28)

For the simplified exponential model this leads to the expression for the radius of curvature as

$$\rho \approx \left[\frac{1+10^{-6}N_s\, e^{\frac{-(h-h_s)}{H_b}}}{\left(\frac{10^{-6}N_s}{H_b}\, e^{\frac{-(h-h_s)}{H_b}}\right)\cos\psi}\right] \approx \left[\frac{1}{\left(\frac{10^{-6}N_s}{H_b}\, e^{\frac{-(h-h_s)}{H_b}}\right)\cos\psi}\right]. \tag{29}$$

We know that ψ depends on altitude, but we also know that it doesn't vary too much around some nominal value from aircraft to target. Consequently, this expression can be reasonably simplified to either of the following approximations

$$\rho \approx \left[\frac{1}{\left(\frac{10^{-6}N_s\cos\psi_g}{H_b}\, e^{\frac{-(h-h_s)}{H_b}}\right)}\right] \approx \left[\frac{1}{\left(\frac{10^{-6}N_s\cos\psi_d}{H_b}\, e^{\frac{-(h-h_s)}{H_b}}\right)}\right]. \tag{30}$$

Now, the instantaneous value for *k* is calculated from the instantaneous value of ρ as

$$k = \frac{1}{1-\left(\frac{R_e}{\rho}\right)}. \tag{31}$$

What we really need, however, is some single average value for *k*. Once we have this value for *k*, we can use the relationships between range, depression angle, and grazing

angle presented in earlier sections. We specifically recall the calculation of depression and grazing angles from propagation path range, repeated here as

$$\sin\psi_d = \frac{(h_a - h_s)}{R}\left(1 - \frac{(h_a - h_s)}{2(kR_e + h_a)}\right) + \frac{R}{2(kR_e + h_a)}, \text{ and}$$
$$\sin\psi_g = \frac{(h_a - h_s)}{R}\left(1 + \frac{(h_a - h_s)}{2(kR_e + h_s)}\right) - \frac{R}{2(kR_e + h_s)}. \quad (32)$$

We do note that these angle equations depend on k, which in turn depends on radius of curvature ρ, which in turn depends on the angles again. Since we often will desire to calculate these angles, or some other geometric parameter based on them, an acceptable solution for k may need to accommodate this.

One option for the calculation of k is to assume that in the absence of any further information, we simply assume a negligibly small angle that allows substituting the cosine term with unity for the calculation of radius of curvature ρ. This, of course, will induce ever larger errors as the angles become more steep. The tolerance to these errors will have to be assessed.

Alternately, we may iterate between calculating k and the angle, until convergence to a mutually satisfactory solution.

3.2.1 The Constant 4/3 Earth Model

At lower altitudes, the segmented Bean and Thayer model degenerates to merely a linear dependence of refractivity on altitude. Near the surface, for a value of N_s = 300, we calculate

$$k \approx \frac{4}{3}. \quad (33)$$

While this is an oft-quoted approximation, it was developed for terrestrial essentially ground-to-ground transmission, and not necessarily airborne radar systems, or radar systems designed for airborne targets.

But even for this atmosphere, for significant h and ψ_g, and non-nominal N_s, the approximation k = 4/3 becomes less and less tenable.

3.2.2 Estimation Method 1 – Average k

As stated, the instantaneous value for k is calculated as

$$k = \frac{1}{1-\left(\frac{R_e}{\rho}\right)} \approx \frac{1}{1-\left(\frac{10^{-6} N_s \cos\psi_g R_e}{H_b}\right) e^{\frac{-(h-h_s)}{H_b}}}. \tag{34}$$

Our first idea is to compute an average value for k, over the altitudes of propagation, as

$$k_{avg} = \frac{1}{(h_a - h_s)} \int_{h_s}^{h_a} k \, dh \approx \left(\frac{H_b}{h_a - h_s}\right) \ln\left(\frac{e^{\frac{(h_a-h_s)}{H_b}} - \frac{10^{-6} N_s \cos\psi_g R_e}{H_b}}{1 - \frac{10^{-6} N_s \cos\psi_g R_e}{H_b}} \right). \tag{35}$$

This expression is certainly more complicated, but at least we have a dependence on aircraft height and surface atmospheric conditions. The question remains "How good is it?" We defer the answer to this for the moment.

3.2.3 Estimation Method 2 – Average Radius of Curvature

If instead we first calculate the average radius of curvature as

$$\rho_{avg} = \frac{1}{(h_a - h_s)} \int_{h_s}^{h_a} \rho \, dh \quad \approx \left(\frac{H_b}{10^{-6} N_s \cos\psi_g}\right) \left(\frac{e^{\frac{(h_a-h_s)}{H_b}} - 1}{\frac{(h_a - h_s)}{H_b}} \right), \tag{36}$$

we can then use it to calculate

$$k_{avg} = \frac{1}{1-\left(\frac{R_e}{\rho_{avg}}\right)} \approx \frac{1}{1-\left(\frac{10^{-6} N_s \cos\psi_g R_e}{H_b}\right) \left(\frac{\frac{(h_a - h_s)}{H_b}}{e^{\frac{(h_a-h_s)}{H_b}} - 1} \right)}. \tag{37}$$

Here we have a similar dependence on aircraft height and surface atmospheric conditions. We still have the question "How good is it?" which we also defer.

These equations for k_{avg} are plotted for $h_s = 0$, and the $N_s = 313$ in Figure 8.

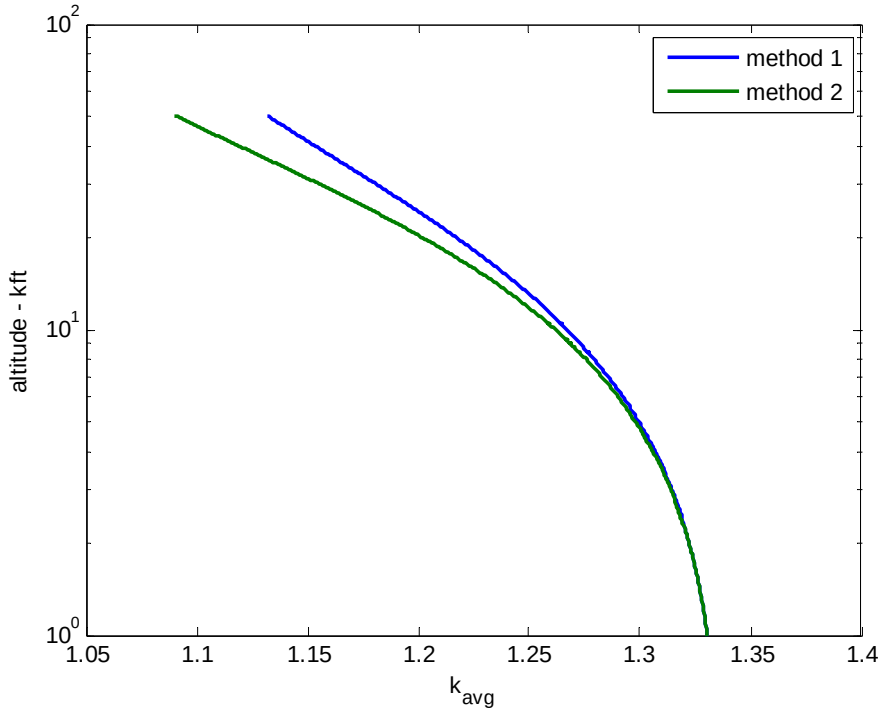

Figure 8. Estimate of variation of k_{avg} with aircraft altitude.

While these two methods give different results, they nevertheless are very similar. Clearly, as altitude increases, both show that the refraction is less, that is, the radius of ray curvature increases and bending decreases, resulting in less modification to the earth's radius. This is good.

We still, however, reasonably ask "Is this any better than the 4/3 earth model?" and "By how much?" We also want to know "Is it worth it?"

3.3 Numerical Integration

Solving for the exact bending vs. range is pretty tough, even if the atmosphere is known, and is typically handled by numerical integration. Following the development in Bean and Dutton, for a spherically stratified atmosphere, we may state Snell's law for polar coordinates with the equation

$$(\tan\psi)\,d\psi = \left(\frac{1}{R_e + h} + \frac{1}{n}\frac{dn}{dh}\right)dh \tag{38}$$

where ψ is the instantaneous elevation angle, and h is the instantaneous altitude above nominal earth's radius. We observe that there is a term that is due to the spherical earth, and a term that is due to refraction itself.

By integrating both sides, we may arrive at the expression

$$-\ln\left(\frac{\cos\psi_d}{\cos\psi_g}\right)=\ln\left(\frac{R_e+h_a}{R_e+h_s}\right)+\int_{h_s}^{h_a}\left(\frac{1}{n}\frac{dn}{dh}\right)dh\,. \tag{39}$$

Completing the integration of the refractivity term may require numerical integration, especially for the most accurate models. Once completed, however, we have a relationship between $\cos\psi_d$ and $\cos\psi_g$. This is done using the segmented Bean and Thayer model in Figure 9, which plots the difference in depression angle and grazing angle as a function of height for various reference atmospheres and grazing angles. Note that from the plot we see that the worst conditions are for the shallowest grazing angles. Clearly some of this is due to the curved earth, and some due to refraction.

If we use the single exponential model for refractivity, this yields

$$\int_{h_s}^{h_a}\left(\frac{1}{n}\frac{dn}{dh}\right)dh=\ln\left(\frac{1+10^{-6}N_s e^{\frac{-(h_a-h_s)}{H_b}}}{1+10^{-6}N_s}\right). \tag{40}$$

These equations may be combined to yield the relationship

$$\frac{\cos\psi_d}{\cos\psi_g}=\left(\frac{1+10^{-6}N_s}{1+10^{-6}N_s e^{\frac{-(h_a-h_s)}{H_b}}}\right)\left(\frac{R_e+h_s}{R_e+h_a}\right). \tag{41}$$

While this neatly relates depression angle to grazing angle as a function of altitude, it relates neither one to the actual propagation path range.

We remind ourselves that our aim is to calculate grazing angle and depression angle for a specified range, and given radar and target heights. We state here the results from Bean and Dutton[4] that the "slant range", which is actually the range (line integral) along the curved propagation path, is calculated from the instantaneous angles as

$$R=\int_{h_s}^{h_a}\left(\frac{1}{\sin\psi}\right)dh=\int_{h_s}^{h_a}\left(\frac{1}{\sqrt{1-\cos^2\psi}}\right)dh\,, \tag{42}$$

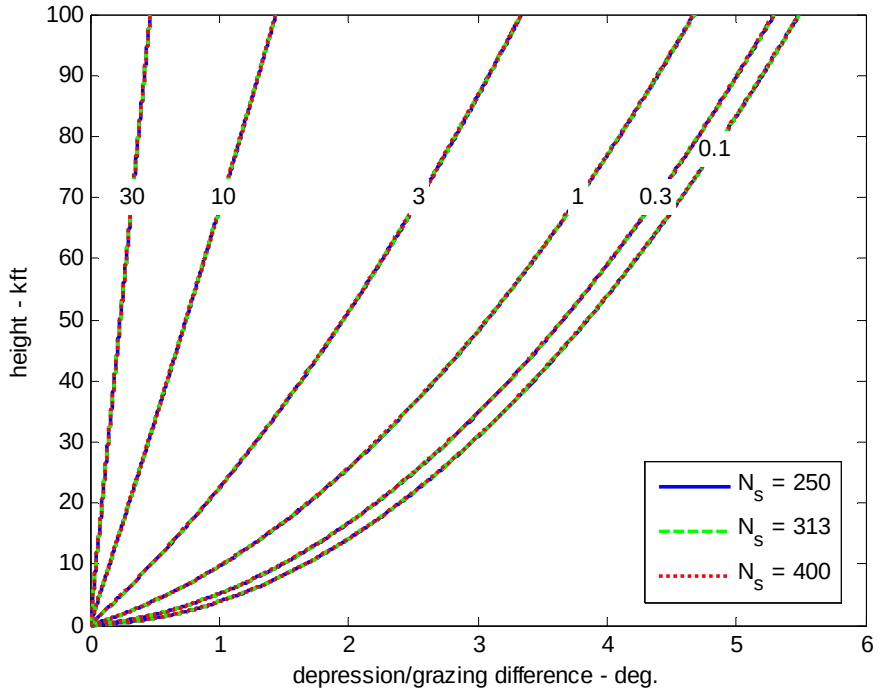

Figure 9. Relationship of depression angle to grazing angle, as function of aircraft altitude for various grazing angles and atmospheres. Curves are labeled with grazing angle in degrees.

where, most precisely the instantaneous angle is related to the refractivity versus height and earth curvature as

$$\cos\psi = \cos\psi_g e^{-\int_{h_s}^{h}\left(\frac{1}{R_e+h'}+\frac{1}{n}\frac{dn}{dh'}\right)dh'} = \cos\psi_g\left(\frac{R_e+h_s}{R_e+h}\right)e^{-\int_{h_s}^{h}\left(\frac{1}{n}\frac{dn}{dh'}\right)dh'}. \qquad (43)$$

Of course we actually want to begin with radar height, target height, and slant range, and therefrom calculate grazing angle and depression angle.

Furthermore, the ground distance at the altitude of the target is calculated as

$$d = \int_{h_s}^{h_a}\left(\frac{R_e+h_s}{R_e+h}\right)\left(\frac{1}{\tan\psi}\right)dh = \int_{h_s}^{h_a}\left(\frac{R_e+h_s}{R_e+h}\right)\left(\frac{\cos\psi}{\sqrt{1-\cos^2\psi}}\right)dh. \qquad (44)$$

3.3.1 Iterative Numerical Integration

The above development allows us to begin with a grazing angle, and therewith calculate a range and depression angle, albeit with numerical integration techniques to achieve the greatest accuracy. We in fact desire to begin with range and respective radar and target altitudes, and therefrom calculate the depression and grazing angles.

One way to do this is to begin with the proper input altitudes, and guess at a set of grazing angles in the neighborhood of the final answer, and calculate corresponding ranges. With such a set, we can then interpolate to the final answer.

Another way to converge arbitrarily close to the final answer is with iterative techniques. We present as example the following algorithm, wherein we will use numerical integration to calculate a relationship between grazing angle and depression angle, and then more numerical integration to calculate range along the curved ray path.

Step 1.

We enter the calculations with input values for

N_s = surface refractivity,
h_a = radar altitude,
h_s = target altitude, and
R = desired propagation path range. (45)

We also select a model for refractivity as a function of height, that is

$N(h)$ = model of refractivity as a function of altitude. (46)

We also select some iteration parameters as

$\Delta\psi_g$ = grazing angle offset for derivative estimation, and
μ = convergence parameter.

Step 2.

We estimate an initial grazing angle as

$$\sin\hat{\psi}_g = \frac{(h_a - h_s)}{R'}\left(1 + \frac{(h_a - h_s)}{2(kR_e + h_s)}\right) - \frac{R'}{2(kR_e + h_s)} \tag{47}$$

where k is estimated in some fashion, perhaps from either method 1 or method 2. Even a constant in the range of 1.0 to 1.3 should work.

Step 3.

Calculate the ratio of cosines as a function of altitude as

$$G(h) = \left(\frac{R_e + h_s}{R_e + h} \right) e^{-\int_{h_s}^{h} \left(\frac{1}{n} \frac{dn}{dh'} \right) dh'} . \tag{48}$$

This calculation is the first numerical integration.

Step 4.

We calculate the instantaneous ray angles as a function of altitude as

$$\begin{aligned} &\cos\psi_0 = G(h)\cos\left(\hat{\psi}_g\right), \\ &\cos\psi_1 = G(h)\cos\left(\hat{\psi}_g - \Delta\psi_g/2\right), \text{ and} \\ &\cos\psi_2 = G(h)\cos\left(\hat{\psi}_g + \Delta\psi_g/2\right). \end{aligned} \tag{49}$$

Furthermore, we calculate the corresponding ranges as

$$\begin{aligned} R_0 &= \int_{h_s}^{h_a} \left(\frac{1}{\sqrt{1 - \cos^2\psi_0}} \right) dh, \\ R_1 &= \int_{h_s}^{h_a} \left(\frac{1}{\sqrt{1 - \cos^2\psi_1}} \right) dh, \text{ and} \\ R_2 &= \int_{h_s}^{h_a} \left(\frac{1}{\sqrt{1 - \cos^2\psi_2}} \right) dh. \end{aligned} \tag{50}$$

This group is the second numerical integration. This allows us to calculate the iteration parameters as

$$\begin{aligned} m &= \frac{R_2 - R_1}{\Delta\psi_g}, \text{ and} \\ \varepsilon &= R_0 - R. \end{aligned} \tag{51}$$

Step 5.

We now update our estimate of the grazing angle as

$$\hat{\psi}_g \leftarrow \hat{\psi}_g - \mu \frac{\varepsilon}{m}. \tag{52}$$

Step 6.

With the new estimate for grazing angle we need to test for convergence.

> If we have converged to a solution,
> then move forward to Step 7,
> else return to Step 4.

A reasonable convergence criterion is that the range error ε is less than some acceptable limit.

Step 7.

The final step is to calculate the depression angle at the radar as

$$\cos\hat{\psi}_d = G(h_a)\cos(\hat{\psi}_g). \tag{53}$$

This ends the procedure.

At this point we should have converged to a grazing angle, and therewith a corresponding depression angle, for the input ranges and altitudes/heights.

3.3.2 Iterative Numerical Integration with Approximations

The previous algorithm using multiple numerical integrations can be modified somewhat by substituting a model for the refractivity profile that allows a closed form integration in the calculation of the ratio of cosines in step 3. Using a simple exponential model, this allows the substitution of the following for step 3.

Step 3.

Calculate the ratio of cosines as a function of altitude as

$$G(h) = \left(\frac{R_e + h_s}{R_e + h}\right)\left(\frac{1 + 10^{-6} N_s}{1 + 10^{-6} N_s e^{\frac{-(h-h_s)}{H_b}}}\right). \tag{54}$$

This calculation is an approximation to the first numerical integration.

3.4 A Comparison of Models and Methods

In this section we compare the several techniques discussed previously. We recall the different models as follows.

Iterative numerical integration

This technique will be our baseline or truth to which we compare the other techniques. It uses the segmented model for refractivity versus height proposed by Bean and Thayer. It then iterates to find the grazing angle best suited to the input propagation path range, and calculates depression angle from the result.

Iterative numerical integration with approximation

This is identical to the iterative numerical integration technique except that a simple single-exponential model is used for refractivity versus height. Specifically, we will use the simple model with a convergence point at 40 kft.

Geometric earth model

This model presumes no refraction at all. It merely assumes straight-line propagation over a spherical earth. This is (nearly) the present model presumed by many radars for pointing the antenna.

4/3 earth model

This is the common technique initially discussed whereby refraction is compensated by presuming a geometry where the earth's radius is increased by a constant factor $k = 4/3$.

Method 1 – average k – Bean and Thayer simple model

This was discussed as method 1. Specifically, for this case, we will use the simple single-exponential model proposed by Bean and Thayer for refractivity as a function of altitude, and calculate an average value of *k* that corresponds to this.

Method 1 – average k

This was discussed as method 1. Specifically, for this case, we will use the simple single-exponential model for refractivity as a function of altitude, but with the convergence point at 40 kft, and calculate an average value of *k* that corresponds to this.

Method 2 – Average radius of curvature

This was discussed as method 2. It averages the refraction radius of curvature over altitude using the simple single-exponential model for refractivity as a

function of altitude, but with the convergence point at 40 kft, and then uses the average curvature to calculate an appropriate earth radius factor *k*.

The next several figures show the error in computed depression angle for a variety of atmospheres and propagation path ranges. Several points become obvious.

- Depression angle inaccuracies are worse for shallow grazing angles.
- The 4/3 earth model is only better than assuming no refraction at all for steeper depression angles, lower altitudes, and more refractive atmospheric conditions. Especially at the higher altitudes and shallower depression angles, the 4/3 earth model yields a worse depression angle estimate.
- The average radius of curvature model (method 2) is generally better than the average *k* model (method 1). Either one of these is usually better than the 4/3 earth model.
- The iterative numerical integration with approximation technique matched the presumed truth the best. (No surprise there.) Usually not far behind is the average radius of curvature model (method 2).

Clearly, which model to use depends on the pointing accuracy desired for the antenna, as well as the availability of atmospheric model parameters.

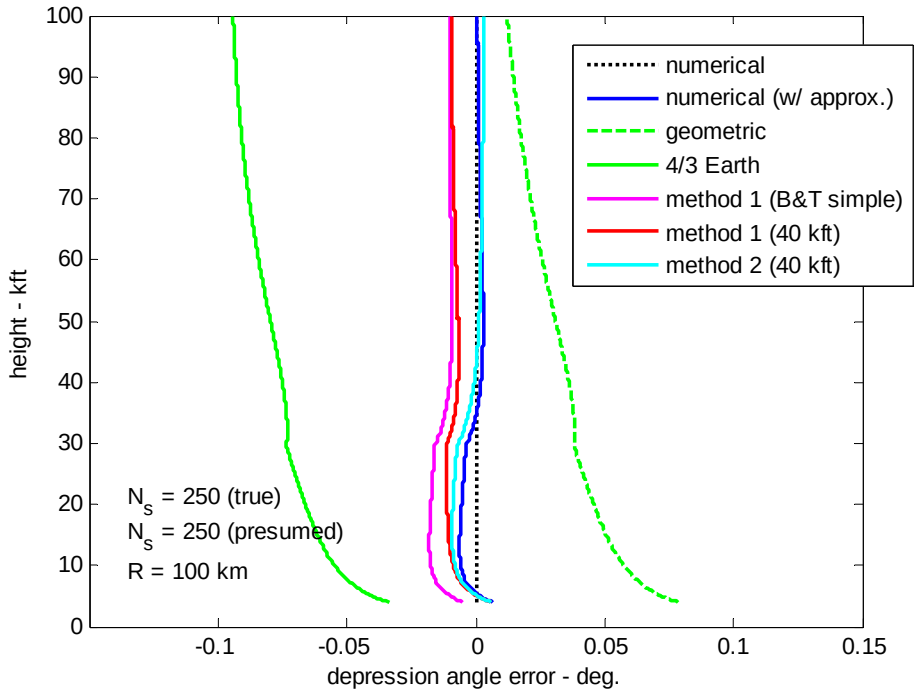

Figure 10. Depression angle error vs. altitude.

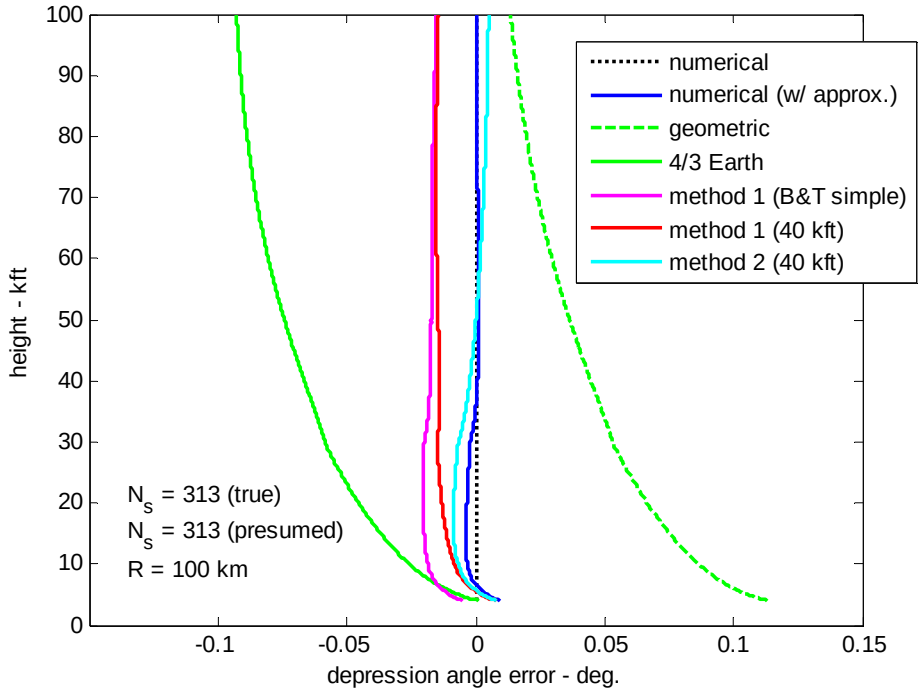

Figure 11. Depression angle error vs. altitude.

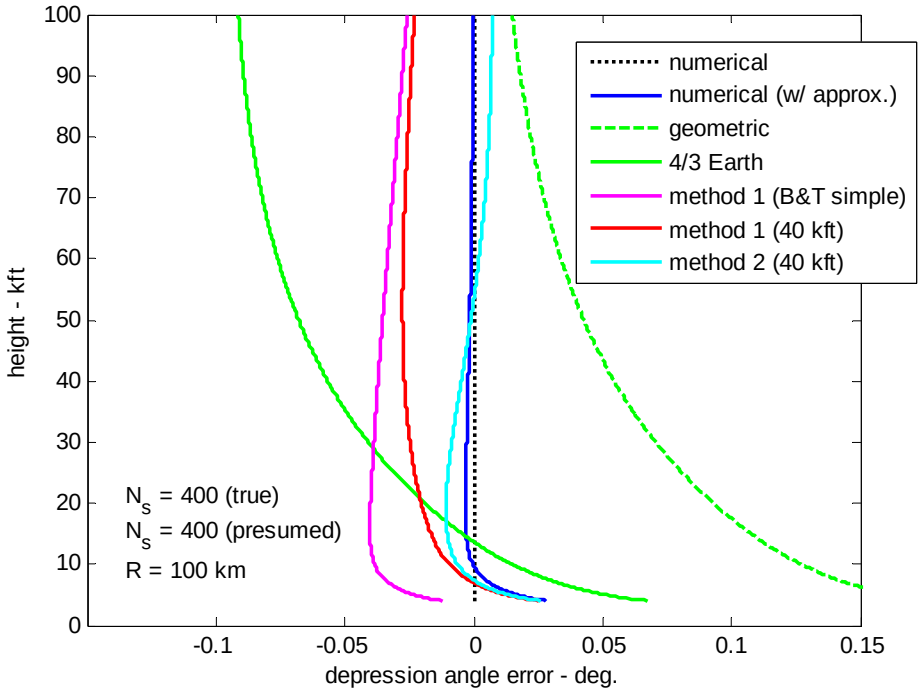

Figure 12. Depression angle error vs. altitude.

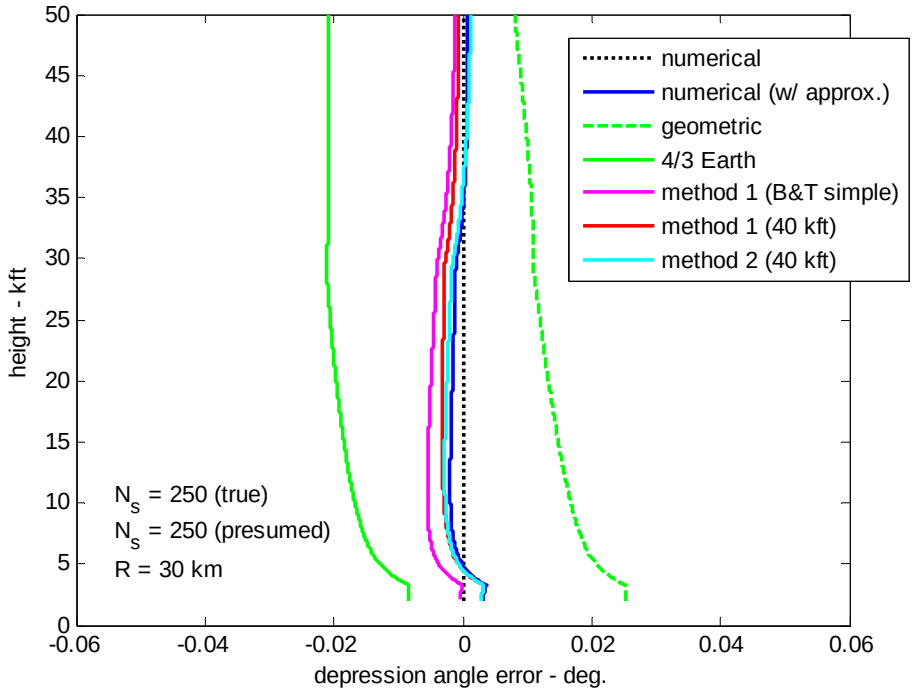

Figure 13. Depression angle error vs. altitude.

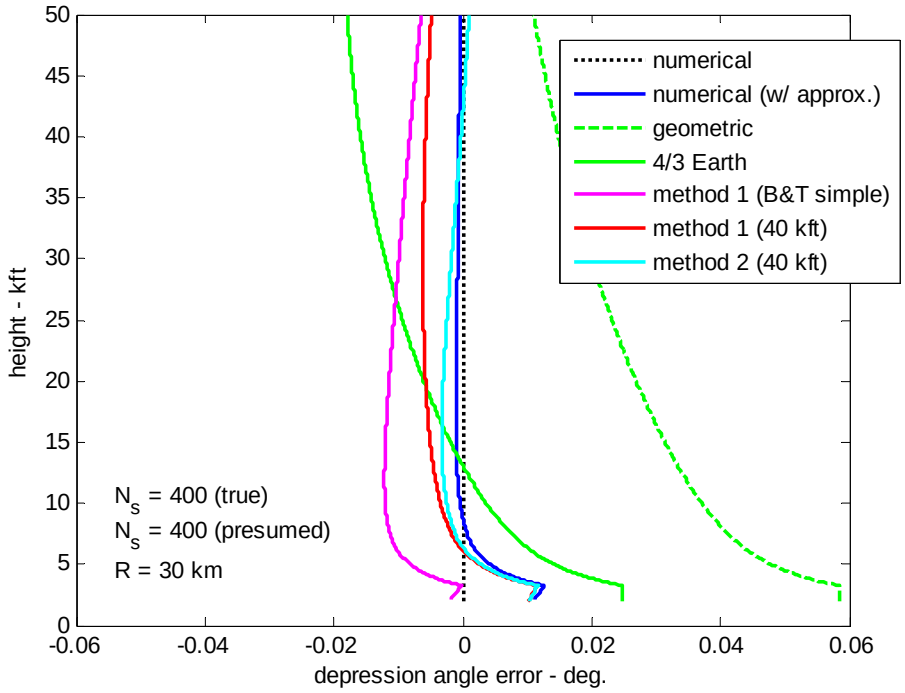

Figure 14. Depression angle error vs. altitude.

What if we don't know the atmosphere, or we don't know N_s?

If we know the exact nature of the atmosphere for all altitudes, we could determine all angles and ranges with maximum accuracy and precision. Since we don't know the atmosphere that accurately, we must rely on models, based perhaps on averages calculated from surface conditions. We have done this up to now in this report.

But now we ask "What if we don't even know the surface conditions?"

The reasonable answer might be to presume some average surface condition, and the attendant average atmosphere, say the $N_s = 313$ reference atmosphere. This leads to the question "Well, how good is that?"

The next several plots show the effect of guessing a wrong N_s.

Based on these plots, several comments come to mind.

- Guessing a wrong reference atmosphere will generally (but not absolutely always) degrade those depression angle estimates that depend on atmospheric parameter inputs. Duh.
- Even the degraded models and methods that presume some nominal reference atmosphere will normally perform better over a larger parameter space than the 4/3 earth model, or the strictly geometric model.
- Among the models that presumed the nominal reference atmosphere, the iterative numerical integration with approximation technique performed roughly comparable to the average radius of curvature technique (method 2), both of which generally performed better than the average *k* technique (method 1).

In other words, even if we guess wrong about atmospheric parameters, those techniques and methods that depend on atmospheric parameters will still generally perform better than those methods that do not. Furthermore, the best techniques are generally the same techniques that are best whether we guess right or guess wrong (probably as long as our wrong guess is not too wrong).

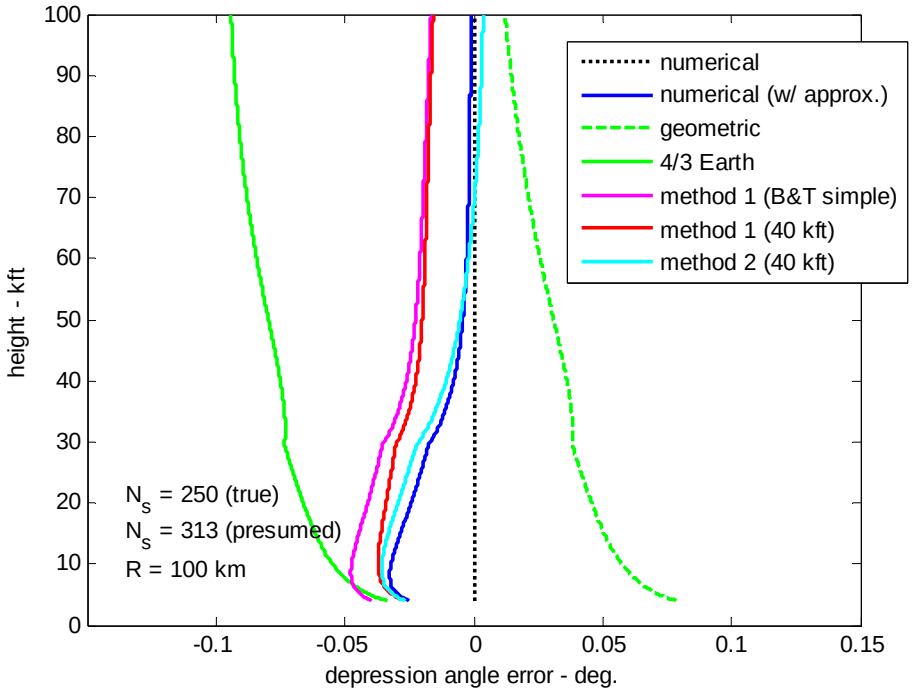

Figure 15. Depression angle error vs. altitude.

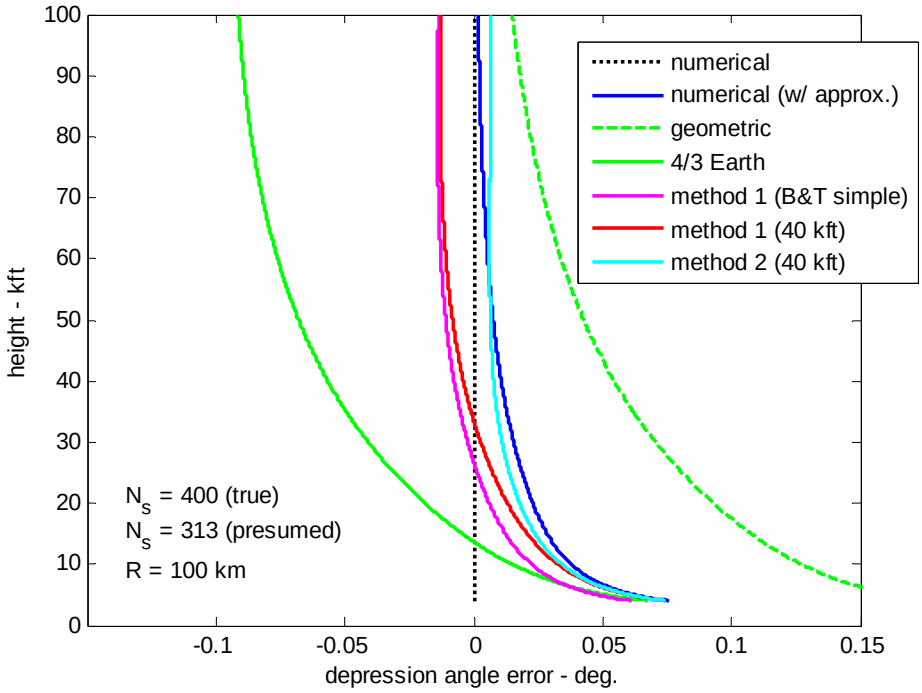

Figure 16. Depression angle error vs. altitude.

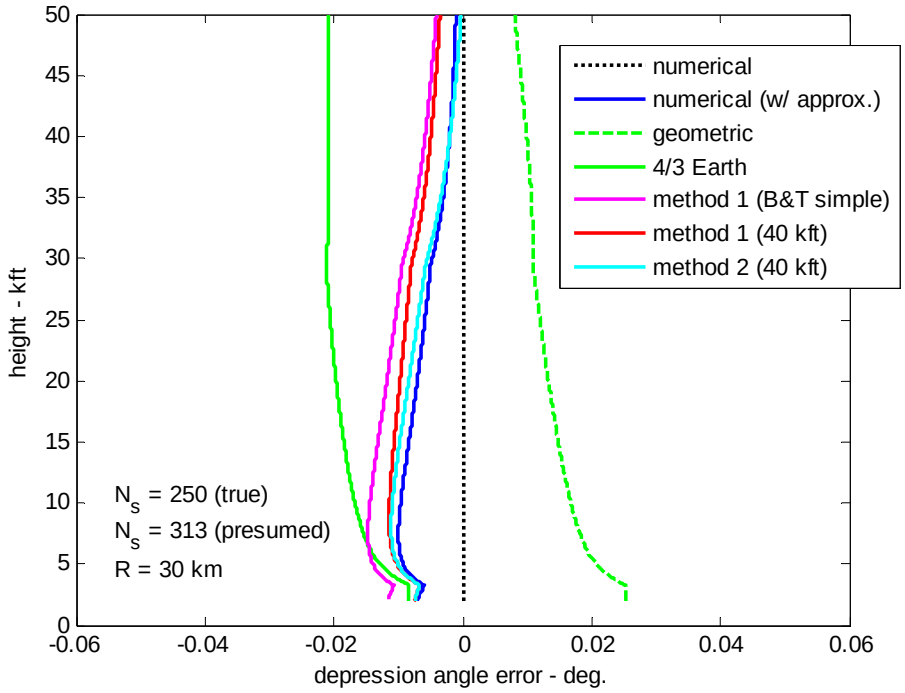

Figure 17. Depression angle error vs. altitude.

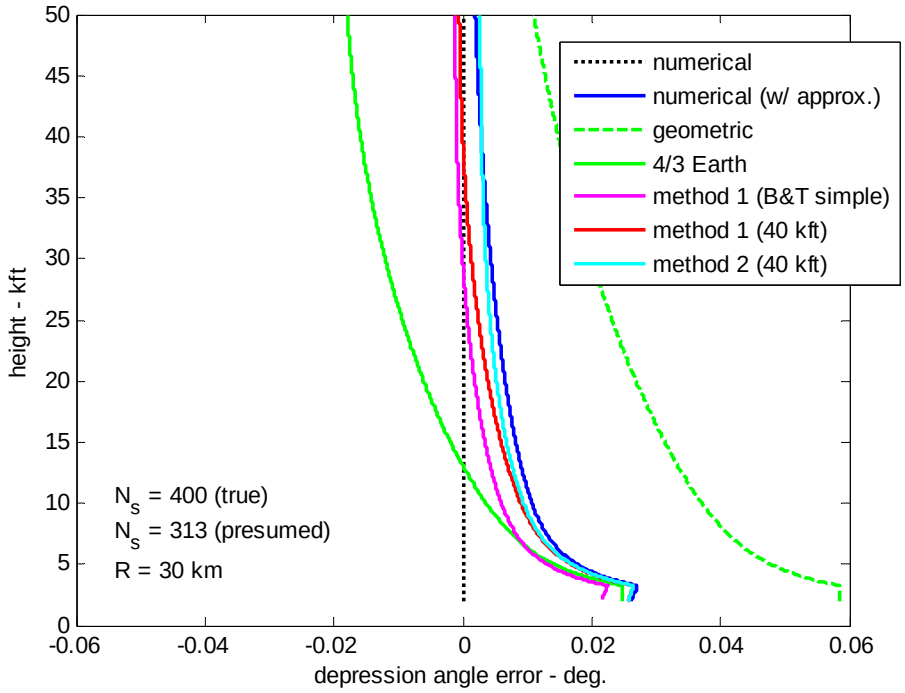

Figure 18. Depression angle error vs. altitude.

3.5 Recommendations

So, the question becomes “Which model do we use when?”

Everything depends, of course, on the pointing accuracy required.

It seems reasonable that if computing time and horsepower exists, the best choice is the iterative numerical integration technique. If a single formula is required, the next best calculation is the average radius of curvature technique (method 2). In both cases, we should use the best guess of the atmospheric parameters. In the absence of specific atmospheric parameters, we should use nominal values, say, the reference atmosphere.

The 4/3 earth model should be used only at very low altitudes.

3.6 More Discussion

Velocity of propagation

The refractivity of the atmosphere also leads to range measurement errors due to the diminished velocity of propagation. To do justice to this topic is beyond the scope of this report, although we will offer here that a radar range measurement is more affected by the ‘slowing’ of the velocity of propagation than by the ‘bending’ of the propagation path. We expect to address this in a future report, and consequently won’t mention it anymore here.

Measuring the required depression angle

Picking the right depression angle to point an antenna means figuring out the proper direction of arrival of the reflected wavefronts. This can be done at least two different ways. The first is acquiring a detailed atmospheric profile of the region of operation, and calculating the exact bending to be compensated or mitigated. The second way is to actually measure the arrival direction of energy from the range of interest, by means of some sort of interferometric technique (e.g. monopulse). The idea is to lock the depression angle to the direction of the clutter return. Of course, if the elevation beamwidth is wide enough, all this is moot.

Which angle to use when

There are two angles to consider in the propagation path. The first is the depression angle, and the second is the grazing angle. Many radars presume these to be equal, both to each other, and to the geometric grazing angle. As this report indicates, both of these presumptions are in error to various extents.

The depression angle is important to pointing the antenna, as we have indicated. Getting this right may be the difference between collecting useable radar data, and no useable radar data at all.

The grazing angle is also important, but to different aspects of the radar, as follows.

- Both clutter reflectivity, as well as clutter RCS, depend on the actual grazing angle.
- The mapping of slant-range resolution and distances to ground-range resolution and distances depends on the actual grazing angle.
- Proper motion compensation, which attempts to stabilize the wavenumber projection onto the ground, also depends on actual grazing angle.

Getting the grazing angle right is more of a data quality issue.

4 Conclusions

The following comments are offered.

- Long range radars especially should include the effects of earth curvature in calculating depression angle and grazing angle. These two will be increasingly different at increasing ranges, mainly because of shallower angles.

- Earth curvature and atmospheric refraction impact not only antenna pointing, but maximum ranges, range scaling, and perhaps clutter reflectivity calculations. Of the two, earth curvature usually has a greater effect than refraction.

- Although many radar systems account for earth curvature, fewer accommodate atmospheric refraction. This amounts to presuming that $k = 1.0$ instead of something larger, say, $k = 4/3$. This hasn't bothered many radar systems in the past because the pointing error tends to be a small fraction of the typical antenna elevation beamwidth.

  In addition, a number of current radar systems use the geometric grazing angle for all motion compensation tasks. Errors because of this are picked up and compensated by autofocus.

- Better models and methods exist to compensate and mitigate the effects of refraction than the $k = 4/3$ earth radius model. These are given in this report.

- IFSAR absolute height accuracy probably needs to account for atmospheric refraction, even at relatively short ranges. Estimates (or presumptions) of local atmospheric conditions (especially surface temperature, pressure, and humidity) should at least be recorded in IFSAR auxiliary data.

- Local atmospheric conditions can cause all sorts of weird anomalous propagation, such as ducting. This was ignored in this report.

- Accurately pointing a high-gain, narrow-beamwidth antenna, especially from space, probably requires a more rigorous analysis that includes other factors such as the ionosphere, etc.

“We all live under the same sky, but we don't all have the same horizon”
-- Konrad Adenauer

References

[1] Armin W. Doerry, “Depression and Grazing Angles with Earth Curvature and Refraction”, Sandia Internal Memorandum, SAND99-2241, September 1999.

[2] Merrill I. Skolnik, *Introduction to Radar Systems - second edition*, ISBN 0-07-057909-1, McGraw-Hill, Inc., 1980.

[3] Bradford R. Bean, “The Radio Refractive Index of Air”, *Proceedings of the I.R.E.*, Vol. 50, Issue 3, pp. 260-273, March 1962.

[4] B. R. Bean, E. J. Dutton, *Radio Meteorology*, National Bureau of Standards Monograph 92, Central Radio Propagation Laboratory, National Bureau of Standards, March 1, 1966.

[5] Earnest K. Smith, Jr., Stanley Weintraub, “The Constants in the Equation for Atmospheric Refractive Index at Radio Frequencies”, *Proceedings of the I.R.E.*, Vol. 4, Issue 8, pp. 1035-1037, August 1953.

[6] B. R. Bean, G. D. Thayer, “Models of the Atmospheric Radio Refractive Index”, *Proceedings of the I.R.E.*, Vol. 45, Issue 5, pp. 740-755, May 1959.

[7] Fred M. Dickey, Armin W. Doerry, Louis A. Romero, “Degrading effects of the lower atmosphere on long range airborne SAR imaging”, *IET Proceedings on Radar, Sonar & Navigation*, Vol. 1, No. 5, pp. 329–339, October 2007.

[8] Bradford R. Bean, “Some Meteorological Effects on Scattered Radio Waves”, *IRE Transactions on Communications Systems*, Vol. 4 , Issue 1, pp. 32-38, March 1956.

[9] B. R. Bean, B. A. Cahoon, C. A. Samson, G. D. Thayer, *A World Atlas Of Atmospheric Radio Refractivity*, Environmental Science Services Administration Monograph 1, Institute for Environmental Research, US Department of Comemrce, 1966.

[10] Edward E. Altshuler, “Tropospheric Range-Error Corrections for the Global Positioning System”, *IEEE Transactions on Antennas and Propagation*, Vol. 46, No 5, pp. 643-649, May 1998.

[11] Simon Kingsley, Shaun Quegan, *Understanding Radar Systems*, ISBN 0-07-707426-2, McGraw-Hill, Inc., 1992.

Distribution

Unlimited Release

1	MS 0532	J. J. Hudgens	5240	
1	MS 0519	J. A. Ruffner	5349	
1	MS 0519	A. W. Doerry	5349	
1	MS 0519	L. Klein	5349	
1	MS 0899	Technical Library	9536	(electronic copy)

;-)